

Effect of phonon coupling on the cooperative two-photon emission from two quantum dots

J. K. Verma, Harmanpreet Singh, and P. K. Pathak

School of Basic Sciences, Indian Institute of Technology Mandi, Kamand, H.P. 175005, India

(Received 13 February 2018; revised manuscript received 27 June 2018; published 12 September 2018)

We predict dominating cooperative two-photon emission from two quantum dots coupled with a single-mode photonic crystal cavity. The cooperative two-photon emission occurs when excitons in two off-resonantly coupled quantum dots decay simultaneously. The interaction with a common cavity field leads to cavity-induced two-photon emission which is strongly inhibited by electron-phonon coupling. The interaction with a common phonon bath produces phonon-induced two-photon emission which increases on increasing temperature. For identical quantum dots, cavity-induced two-photon emission is negligible, but phonon-induced two-photon emission could be large.

DOI: [10.1103/PhysRevB.98.125305](https://doi.org/10.1103/PhysRevB.98.125305)**I. INTRODUCTION**

Cooperative emission by an ensemble of N identical two-level atoms has been the subject of intense theoretical and experimental research after the discovery of superradiance by Dicke [1]. It has been shown that the initial state as a symmetric superposition of atomic states leads to superradiance, whereas antisymmetric superpositions of atomic states get decoupled from the environment and radiate negligible intensity [2]. Such interesting effects arise due to quantum interference between different possible atomic transitions [3]. The superradiant and subradiant behavior has also been observed in the cooperative emission of two emitters [3,4] in a cavity. Further, the concept of superradiance and subradiance has been extended to the inhomogeneously broadened ensembles such as densely spaced semiconductor quantum dots (QDs) coupled to a microcavity [5].

Recently, there have been considerable interests in developing on-chip photonic circuits using QDs coupled with photonic crystal microcavities and waveguides, particularly for the purpose of scalable quantum information processing [6]. Owing to strong electrons and holes confinement, QDs have atomlike discrete energy levels and with current technology it is possible now to deterministically position a QD at a desired position in photonic crystal microcavities with very high accuracy [7]. Significant technological progress has been made in realizing these systems, e.g., ultrahigh-quality cavities [8] and ultralow-loss waveguides have been designed [9]. Further, incoherent [10] as well as coherent excitation [11] techniques, and strong-coupling regimes in QD-microcavity coupled systems [7,12], have been realized. A two-photon resonant transition in a single QD through biexciton cascaded decay has been observed [13]. A Jaynes-Cummings ladder [14], where more than one photon interaction with a single two-level system becomes significant, has also been observed. Clearly these developments have proved photonic systems as a potential candidate for developing integrated photonic technology and scalable quantum information circuits. However, most of these studies involve interaction of the single QD with an electromagnetic field. In this paper, we consider cooperative two-photon emission from two separated QDs. We

are particularly interested in cooperative two-photon emission from two off-resonant QDs when the probabilities of single-photon emissions could be very small. Dominating two-photon emission occurs when two-photon resonant conditions are satisfied. Under two-photon resonant conditions, possible two-photon transitions become indistinguishable and interfere constructively. The two-photon resonant condition can be satisfied either for two unidentical QDs having different dipole coupling constants and exciton transition frequencies or for two identical QDs having the same dipole coupling constants and exciton transition frequencies. We specifically bring out the role of phonon coupling in cooperative two-photon emission from two QDs. In semiconductor cavity quantum electrodynamics, coupling with a phonon bath is a unique phenomenon which is primarily responsible for exciton dephasing [15]. Other important processes such as off-resonant cavity-mode feeding [16,17], phonon-mediated population inversion [18], and phonon-assisted biexciton generation [19] have also been observed. We notice that there have been some interesting theoretical as well as experimental results demonstrating coupling between two quantum dots induced by a common interacting field [20]. In the system of two QDs, interaction with a common phonon field also plays a significant role and the phonon-mediated coupling between two QDs has been recently observed [21].

Our paper is organized as follows. In Sec. II, we present our model for resonant two-photon emission and a theoretical framework using recently developed master equation techniques [17]. The population dynamics, probabilities for photon emissions, and spectrum of the generated photons is presented in Sec. III. Finally, we conclude in Sec. IV.

II. TWO QDS INTERACTING WITH A SINGLE-MODE CAVITY

We consider two separated QDs embedded in a single-mode photonic crystal cavity. The energy levels of the i th QD are represented by $|g_i\rangle$ and $|e_i\rangle$, for $i = 1, 2$, corresponding to the ground state and exciton state. The Hamiltonian in the

rotating frame is given by

$$H = \hbar\delta_1\sigma_1^+\sigma_1^- + \hbar\delta_2\sigma_2^+\sigma_2^- + \hbar g_1(\sigma_1^+a + a^\dagger\sigma_1^-) + \hbar g_2(\sigma_2^+a + a^\dagger\sigma_2^-) + H_{\text{ph}}, \quad (1)$$

where $\sigma_i^+ = |e_i\rangle\langle g_i|$, $\sigma_i^- = |g_i\rangle\langle e_i|$, $\delta_i = \omega_i - \omega_c$, ω_c is frequency of the cavity mode, ω_i is the transition frequency for the exciton energy level, g_i is the coupling constant for the i th QD, and a and a^\dagger are photon annihilation and creation operators, respectively. The phonon bath and exciton-phonon interaction is included in $H_{\text{ph}} = \hbar \sum_k \omega_k b_k^\dagger b_k + \lambda_k \sigma_1^+ \sigma_1^- (b_k + b_k^\dagger) + \mu_k \sigma_2^+ \sigma_2^- (b_k + b_k^\dagger)$, with b_k (b_k^\dagger) as the phonon annihilation (creation) operator for the k th mode. In order to understand the influence of exciton-phonon interaction we made a polaron transform. The transformed Hamiltonian $H' = e^P H e^{-P}$ with $P = \sigma_1^+ \sigma_1^- \sum_k \frac{\lambda_k}{\omega_k} (b_k - b_k^\dagger) + \sigma_2^+ \sigma_2^- \sum_k \frac{\mu_k}{\omega_k} (b_k - b_k^\dagger)$, which is separated into a cavity-QD system, with phonon bath and system-bath interaction as $H' = H_s + H_b + H_{\text{sb}}$, where

$$H_s = \hbar\Delta_1\sigma_1^+\sigma_1^- + \hbar\Delta_2\sigma_2^+\sigma_2^- + \langle B \rangle X_g, \quad (2)$$

$$H_b = \hbar \sum_k \omega_k b_k^\dagger b_k, \quad (3)$$

$$H_{\text{sb}} = \xi_g X_g + \xi_u X_u, \quad (4)$$

where the polaron shifts $\sum_k \lambda_k^2/\omega_k$, $\sum_k \mu_k^2/\omega_k$ are included in the effective detunings Δ_1 and Δ_2 . The system operators are given by $X_g = \hbar(g_1\sigma_1^+a + g_2\sigma_2^+a) + \text{H.c.}$, $X_u = i\hbar(g_1\sigma_1^+a + g_2\sigma_2^+a) + \text{H.c.}$, and bath fluctuation operators are $\xi_g = \frac{1}{2}(B_+ + B_- - 2\langle B \rangle)$ and $\xi_u = \frac{1}{2i}(B_+ - B_-)$. The phonon displacement operators are $B_\pm = \exp[\pm \sum_k \frac{\lambda_k}{\omega_k} (b_k - b_k^\dagger)] = \exp[\pm \sum_k \frac{\mu_k}{\omega_k} (b_k - b_k^\dagger)]$ with expectation value $\langle B \rangle = \langle B_+ \rangle = \langle B_- \rangle$. We use a transformed Hamiltonian H' to derive the polaron master equation for describing the dynamics of the system. After making the Born-Markov approximation, the master equation is derived in Lindblad form. The Lindblad superoperator corresponding to an operator \hat{O} is defined as $\mathcal{L}[\hat{O}]\rho = \hat{O}^\dagger \hat{O} \rho - 2\hat{O} \rho \hat{O}^\dagger + \rho \hat{O}^\dagger \hat{O}$. The spontaneous emission, cavity damping, and phonon-induced dephasing are also included in the master equation. The final form of the master equation in terms of the density matrix for the cavity-QD coupled system ρ_s is written as [17]

$$\dot{\rho}_s = -\frac{i}{\hbar}[H_s, \rho_s] - \mathcal{L}_{\text{ph}}\rho_s - \frac{\kappa}{2}\mathcal{L}[a]\rho_s - \sum_{i=1,2} \frac{\gamma_i}{2}\mathcal{L}[\sigma_i^-]\rho_s - \frac{\gamma_i'}{2}\mathcal{L}[\sigma_i^+\sigma_i^-]\rho_s, \quad (5)$$

where κ , γ_i , γ_i' are cavity leakage, spontaneous decay, dephasing rates, and

$$\mathcal{L}_{\text{ph}}\rho_s = \frac{1}{\hbar^2} \int_0^\infty d\tau \sum_{j=g,u} G_j(\tau) \times [X_j(t), X_j(t, \tau)\rho_s(t)] + \text{H.c.}, \quad (6)$$

with $X_j(t, \tau) = e^{-iH_s\tau/\hbar} X_j(t) e^{iH_s\tau/\hbar}$, and the polaron Green functions are given by $G_g(\tau) = \langle B \rangle^2 \{\cosh[\phi(\tau)] - 1\}$ and

$G_u(\tau) = \langle B \rangle^2 \sinh[\phi(\tau)]$. In this master equation system-phonon interaction is included in the phonon correlation function $\phi(\tau)$. The phonon bath is treated as a continuum with spectral function $J(\omega) = \alpha_p \omega^3 \exp[-\omega^2/2\omega_b^2]$, where the parameters α_p and ω_b are the electron-phonon coupling and cutoff frequency, respectively. In our calculations we use $\alpha_p = 1.42 \times 10^{-3} g_1^2$ and $\omega_b = 10g_1$, which gives $\langle B \rangle = 1.0, 0.90, 0.84,$ and 0.73 for $T = 0$ K, $T = 5, 10,$ and 20 K, respectively, values which match with recent experiments [17,22]. The phonon correlation function is given by

$$\phi(\tau) = \int_0^\infty d\omega \frac{J(\omega)}{\omega^2} \left[\coth\left(\frac{\hbar\omega}{2K_b T}\right) \cos(\omega\tau) - i \sin(\omega\tau) \right], \quad (7)$$

where K_b and T are the Boltzmann constant and the temperature of the phonon bath, respectively.

We are interested in two-photon cooperative emission from two QDs; therefore we work in the condition where single-photon transitions are suppressed from individual QDs, i.e., the coupling constants of the cavity field with QDs are much smaller than their detunings ($g_1, g_2 \ll \Delta_1, \Delta_2$). Under such conditions the master equation (5) can be further simplified, using $H_s = \hbar\Delta_1\sigma_1^+\sigma_1^- + \hbar\Delta_2\sigma_2^+\sigma_2^-$ and neglecting the terms proportional to g_1 and g_2 in the expression of $X_j(t, \tau)$. The simplified form of the master equation provides a clear picture of processes involved in the dynamics. Under such an approximation the master equation (5) takes the form

$$\begin{aligned} \dot{\rho}_s = & -\frac{i}{\hbar}[H_{\text{eff}}, \rho_s] - \frac{\kappa}{2}\mathcal{L}[a]\rho_s \\ & - \sum_{i=1,2} \left(\frac{\gamma_i}{2}\mathcal{L}[\sigma_i^-] + \frac{\gamma_i'}{2}\mathcal{L}[\sigma_i^+\sigma_i^-] \right. \\ & \left. + \frac{\Gamma_i^-}{2}\mathcal{L}[\sigma_i^+a] + \frac{\Gamma_i^+}{2}\mathcal{L}[a^\dagger\sigma_i^-] \right) \rho_s \\ & - \left[\frac{\Gamma_{12}^-}{2}(\sigma_1^+a\sigma_2^+a\rho_s - 2\sigma_2^+a\rho_s\sigma_1^+a + \rho_s\sigma_1^+a\sigma_2^+a) \right. \\ & + \frac{\Gamma_{12}^{++}}{2}(a^\dagger\sigma_1^-a^\dagger\sigma_2^-\rho_s - 2a^\dagger\sigma_2^-\rho_s a^\dagger\sigma_1^- + \rho_s a^\dagger\sigma_1^- a^\dagger\sigma_2^-) \\ & + \frac{\Gamma_{12}^{+-}}{2}(\sigma_1^+aa^\dagger\sigma_2^-\rho_s - 2a^\dagger\sigma_2^-\rho_s\sigma_1^+a + \rho_s\sigma_1^+aa^\dagger\sigma_2^-) \\ & \left. + \frac{\Gamma_{12}^{+-}}{2}(a^\dagger\sigma_1^-\sigma_2^+a\rho_s - 2\sigma_2^+a\rho_s a^\dagger\sigma_1^- + \rho_s a^\dagger\sigma_1^-\sigma_2^+a) \right. \\ & \left. + 1 \leftrightarrow 2 \right], \quad (8) \end{aligned}$$

where the first term corresponds to the effective dynamics of the system when QDs are far off-resonant. The effective Hamiltonian is given by

$$H_{\text{eff}} = H_s + \hbar \sum_{i=1,2} (\delta_i^- a^\dagger \sigma_i^- \sigma_i^+ a + \delta_i^+ \sigma_i^+ a a^\dagger \sigma_i^-) - (i\hbar\Omega_{2ph}\sigma_1^-\sigma_2^-a^\dagger + \text{H.c.}) - (i\hbar\Omega_+ \sigma_1^+ a a^\dagger \sigma_2^- + i\hbar\Omega_- a^\dagger \sigma_1^- \sigma_2^+ a + \text{H.c.}), \quad (9)$$

where δ_i^\pm are Stark shifts, the third term represents two-photon processes, and the fourth term corresponds to excitation

transfer processes from one QD to another. The expressions for Stark shifts, two-photon transition couplings, and excitation transfer couplings are given by

$$\delta_i^\pm = g_i^2 \Im \left[\int_0^\infty d\tau G_+ e^{\pm i \Delta_i \tau} \right], \quad (10)$$

$$\Omega_{2ph} = \frac{g_1 g_2}{2} \int_0^\infty d\tau (G_- - G_-^*) (e^{-i \Delta_1 \tau} + e^{-i \Delta_2 \tau}), \quad (11)$$

$$\Omega_\pm = \frac{g_1 g_2}{2} \int_0^\infty d\tau (G_+ e^{\pm i \Delta_2 \tau} - G_+^* e^{\mp i \Delta_1 \tau}), \quad (12)$$

with $G_\pm = \langle B \rangle^2 (e^{\pm i \phi(\tau)} - 1)$. The phonon-induced cavity-mode feeding rates Γ_i^\pm , two-photon emission and absorption rates Γ_{ij}^{++} and Γ_{ij}^{--} , and the excitation transfer rates $\Gamma_{ij}^{\pm\mp}$ are given by

$$\Gamma_i^\pm = g_i^2 \int_0^\infty d\tau (G_+ e^{\pm i \Delta_i \tau} + G_+^* e^{\mp i \Delta_i \tau}), \quad (13)$$

$$\Gamma_{ij}^{++} = g_i g_j \int_0^\infty d\tau (G_- e^{i \Delta_j \tau} + G_-^* e^{i \Delta_i \tau}), \quad (14)$$

$$\Gamma_{ij}^{--} = g_i g_j \int_0^\infty d\tau (G_- e^{-i \Delta_j \tau} + G_-^* e^{-i \Delta_i \tau}), \quad (15)$$

$$\Gamma_{ij}^{+-} = g_i g_j \int_0^\infty d\tau (G_+ e^{-i \Delta_j \tau} + G_+^* e^{i \Delta_i \tau}), \quad (16)$$

$$\Gamma_{ij}^{-+} = g_i g_j \int_0^\infty d\tau (G_+ e^{i \Delta_j \tau} + G_+^* e^{-i \Delta_i \tau}). \quad (17)$$

We solve master equation (5) numerically using a quantum optics tool box [23]. In the case when QDs are far off-resonant, the numerical results by using approximated master equation (8) and the results obtained after integration of master equation (5) match perfectly. We relegate the details to the Appendix.

III. RESULTS AND DISCUSSION

For dominating two-photon cooperative emission, we consider QDs are off-resonantly coupled with a cavity mode. Initially both QDs are in exciton states and there is no photon in the cavity mode, i.e., the initial state of the system is $|e_1, e_2, 0\rangle$. In Figs. 1–4, we fix the detuning of one QD, say Δ_1 , and scan the detuning of the other QD for two-photon resonant emission. For subplots (a), (b), (c), and (d), we consider no coupling with a phonon bath, coupling with a phonon bath at $T = 5$ K, coupling with a phonon bath at $T = 10$ K, and coupling with a phonon bath at $T = 20$ K, respectively. We plot photon emission probabilities from state $|g_1, e_2, 1\rangle$, $|e_1, g_2, 1\rangle$, and $|g_1, g_2, 2\rangle$, given by $P = \kappa \int_0^\infty dt \langle g_1, e_2, 1 | \rho_s(t) | g_1, e_2, 1 \rangle$, $Q = \kappa \int_0^\infty dt \langle e_1, g_2, 1 | \rho_s(t) | e_1, g_2, 1 \rangle$, and $R = 2\kappa \int_0^\infty dt \langle g_1, g_2, 2 | \rho_s(t) | g_1, g_2, 2 \rangle$, respectively. It is clear that even g_1 and Δ_1 are fixed, and the probabilities P and R also depend on Δ_2 , which demonstrates that QDs get coupled after interaction with a common cavity field and phonon bath. Further, for small spontaneous decay rates $P + Q + R > 0.8$ for $|\Delta_2| \leq 5g_1$. In Figs. 1 and 2, we consider that the QDs are placed in the cavity such that they have different dipole coupling constants $g_1 \neq g_2$. In Fig. 1(a), when there is no coupling with the phonon bath and the detuning for the first

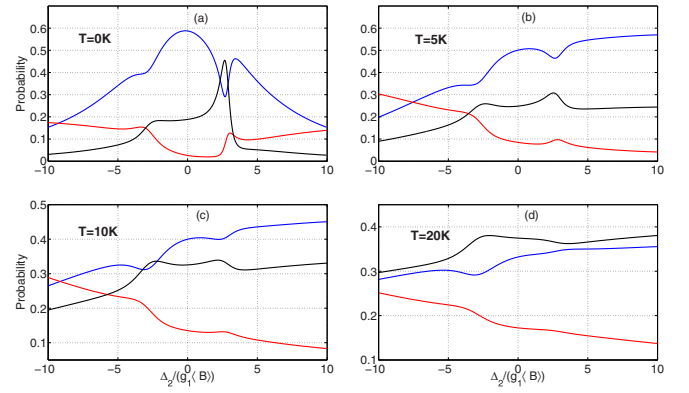


FIG. 1. The probabilities of photon emission, P from state $|g_1, e_2, 1\rangle$ (red line), Q from state $|e_1, g_2, 1\rangle$ (blue line), R from state $|g_1, g_2, 2\rangle$ (black line). The parameters are $g_2 = 2g_1$, $\Delta_1 = -5g_1 \langle B \rangle$, $\kappa = 0.1g_1$, $\gamma_1 = \gamma_2 = \gamma'_1 = \gamma'_2 = 0.01g_1$.

QD is fixed for negative value $\Delta_1 = -5g_1 \langle B \rangle$, the probability P remains small and the probability Q becomes maximum for $\Delta_2 = 0$. The probability Q shows a dip, whereas the probability R shows cavity-induced two-photon resonance for $\Delta_1 + \Delta_2 + 2g_1^2/\Delta_1 + 2g_2^2/\Delta_2 \approx 0$ [24], for $g_2 = 2g_1$ and $\kappa = 0.1g_1$, $\Delta_2 = 2.65g_1 \langle B \rangle$. Further, small values of cavity damping are necessary in order to achieve two-photon processes. The appearance of two-photon resonance in R is a consequence of constructive interference between two-photon transitions $|e_1, e_2, 0\rangle \rightarrow |e_1, g_2, 1\rangle \rightarrow |g_1, g_2, 2\rangle$ and $|e_1, e_2, 0\rangle \rightarrow |g_1, e_2, 1\rangle \rightarrow |g_1, g_2, 2\rangle$ [24]. The cavity-induced two-photon resonance satisfies energy conservation $\Delta_1 + \Delta_2 \approx 0$ when we include Stark shifts. In Fig. 1(b), we include coupling with a phonon bath at $T = 5$ K. The coupling with phonon reduces the interference between two possible photon transitions and thus reduces the probability R at cavity-induced two-photon resonance. When QDs are far off-resonant the phonon-induced cavity-mode feeding enhances single-photon processes and thus P and Q increase. The probability P when the photon is leaked from state $|g_1, e_2, 1\rangle$ and the probability Q when the photon is leaked from state $|e_1, g_2, 1\rangle$ complement each other. When

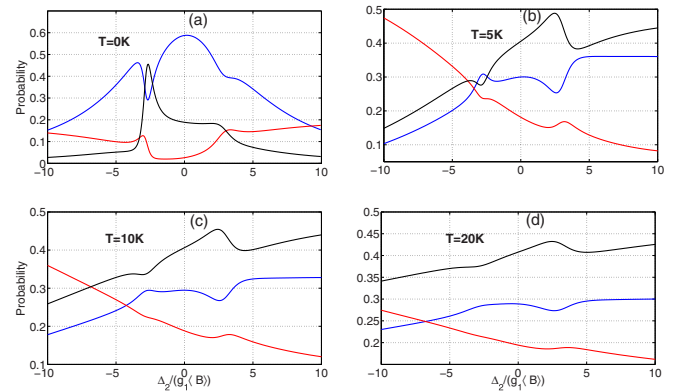


FIG. 2. The probabilities of photon emission, P from state $|g_1, e_2, 1\rangle$ (red line), Q from state $|e_1, g_2, 1\rangle$ (blue line), R from state $|g_1, g_2, 2\rangle$ (black line). The parameters are the same as in Fig. 1, except $\Delta_1 = 5g_1 \langle B \rangle$.

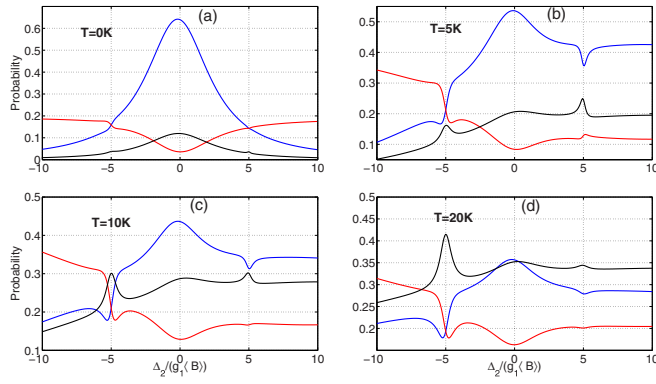


FIG. 3. The probabilities of photon emission, P from state $|g_1, e_2, 1\rangle$ (red line), Q from state $|e_1, g_2, 1\rangle$ (blue line), R from state $|g_1, g_2, 2\rangle$ (black line). The parameters are $g_2 = g_1$, $\Delta_1 = -5g_1\langle B\rangle$, $\kappa = 0.1g_1$, $\gamma_1 = \gamma_2 = \gamma'_1 = \gamma'_2 = 0.01g_1$.

probability P increases, Q decreases and vice versa. When excitons do not decay through single-photon processes, i.e., the photon does not emit from state $|e_1, g_2, 1\rangle$ or $|g_1, e_2, 1\rangle$, two photons are generated in cavity mode and the state of the system is given by $|g_1, g_2, 2\rangle$. Therefore, when R increases P and Q decrease. In Figs. 1(c) and 1(d), when the temperature of the phonon bath increases, two-photon processes increase, leading to larger probability R for all values of Δ_2 . The coupling with the phonon bath also opens up new phonon-induced two-photon resonance. We find, using master equation (8), that the terms corresponding to Γ_{ij}^{+-} and Γ_{ij}^{-+} are responsible for phonon-induced two-photon resonance. These terms correspond to exciton transfer, which dominate when QDs are equally detuned. In the presence of interaction H_s , the effective detunings include Stark shifts. Thus phonon-induced two-photon resonance occurs when $\Delta_1 + 2g_1^2/\Delta_1 \approx \Delta_2 + 2g_2^2/\Delta_2$. In this case the two-photon transitions $e_1, e_2, 0\rangle \rightarrow |e_1, g_2, 1\rangle \rightarrow |g_1, g_2, 2\rangle$ and $e_1, e_2, 0\rangle \rightarrow |g_1, e_2, 1\rangle \rightarrow |g_1, g_2, 2\rangle$ become indistinguishable and interfere constructively again.

In Fig. 2, we fix the detuning of the first QD to positive value $\Delta_1 = 5g_1\langle B\rangle$. In this case the cavity-induced two-photon resonance appears for $\Delta_2 = -2.6g_1\langle B\rangle$ [see Fig. 2(a)]. The probabilities P , Q , and R have the same values as in Fig. 1(a) but for negative values of Δ_2 . In Fig. 2(b), when coupling with the phonon bath at $T = 5$ K is introduced, a prominent phonon-induced two-photon resonance appears for $\Delta_1 + 2g_1^2/\Delta_1 \approx \Delta_2 + 2g_2^2/\Delta_2$. The cavity-induced two-photon resonance which appears without coupling with the phonon bath disappears. The probabilities corresponding to single-photon processes P and Q increase when QDs are far off-resonant. The phonon interaction is asymmetric for positive and negative values of detunings. The asymmetric behavior of phonon interaction has been observed in QD-cavity systems [17,22] earlier. In Figs. 2(c) and 2(d), when the phonon bath temperature is increased from $T = 10$ K to $T = 20$ K, two-photon processes become larger for all values of Δ_2 except at resonance. At two-photon resonance the probability R decreases slightly as P and Q increase slightly around resonance.

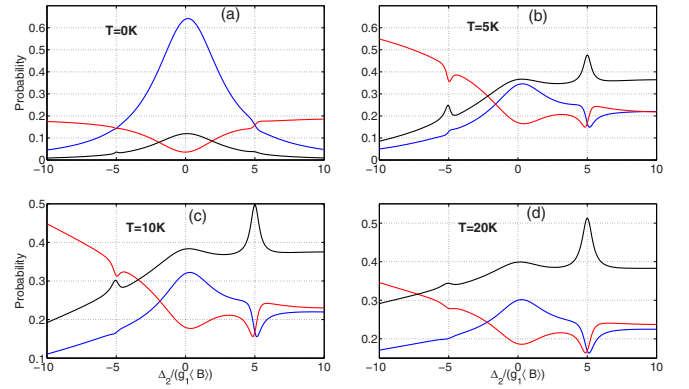


FIG. 4. The probabilities of photon emission, P from state $|g_1, e_2, 1\rangle$ (red line), Q from state $|e_1, g_2, 1\rangle$ (blue line), R from state $|g_1, g_2, 2\rangle$ (black line). The parameters are the same as in Fig. 3, except $\Delta_1 = 5g_1\langle B\rangle$.

In Figs. 3 and 4, we consider both QDs have the same dipole couplings, $g_1 = g_2$. In this case cavity-induced two-photon transitions remain negligible [24] and single-photon transitions dominate, when we do not consider coupling with the phonon bath as shown in Figs. 3(a) and 4(a). In fact, for $g_1 = g_2$, the two possible two-photon transitions interfere destructively, making the probability of generating state $|g_1, g_2, 2\rangle$ negligible. In Fig. 3, we fix detuning of the first QD to negative value $\Delta_1 = -5g_1\langle B\rangle$. When we consider electron-phonon coupling at temperature $T = 5$ K, two-photon processes increase in Fig. 3(b). For positive values of Δ_2 two-photon processes are larger than for negative values of Δ_2 . Further, two tiny peaks appear for $\Delta_2 = \pm\Delta_1$. The peak at $\Delta_2 = \Delta_1$ corresponds to phonon-induced two-photon resonance, and the peak at $\Delta_2 = -\Delta_1$ corresponds to cavity-induced two-photon resonance as the interference conditions change after coupling with the phonon bath. In Figs. 3(c) and 3(d), two-photon processes become more dominating, leading to larger values of R and smaller values of P and Q . At $T = 20$ K, two-photon processes dominate for positive values of Δ_2 , with a dominating resonance for negative value at $\Delta_2 = \Delta_1$. In Fig. 4, we fix $\Delta_1 = 5g_1\langle B\rangle$. In Fig. 4(b), when electron-phonon coupling at 5 K is considered, the two-photon processes increase and dominate over single-photon processes, leading to larger values of R than P and Q for positive Δ_2 . On increasing the temperature, in Figs. 4(c) and 4(d), the two-photon processes become larger and single-photon processes decrease. A dominating phonon-induced two-photon resonance appears at $\Delta_2 = \Delta_1$.

In Figs. 1(a) and 2(a), for $g_1 \neq g_2$ and $T = 0$ K, cavity-mediated two-photon interaction is significant and phonon interaction is absent. When Δ_1 is fixed to a negative (positive) value in Fig. 1(a) [Fig. 2(a)], two-photon resonance occurs for positive (negative) values of Δ_2 . Further, in Figs. 3(a) and 4(a), for $g_1 = g_2$ and $T = 0$ K, cavity-mediated and phonon-mediated two-photon interactions are negligible and the probabilities P , Q , and R are almost symmetric. However at higher temperatures, phonon-mediated two-photon resonance occurs when Δ_1 and Δ_2 are of the same sign. Further, the phonon-induced cavity-mode feeding process followed by emission of the phonon for positive detunings is stronger than

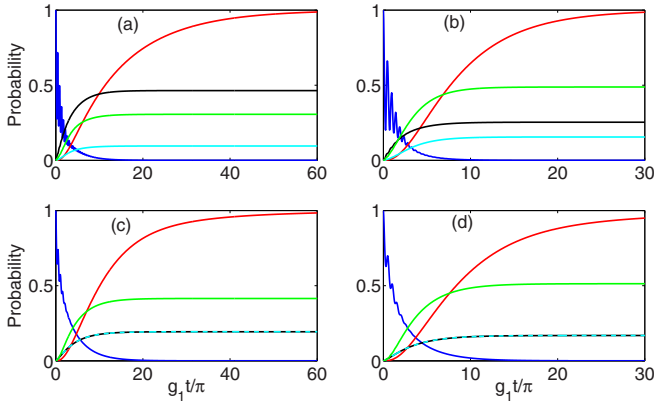


FIG. 5. The density matrix element $\rho_{ee}(t) = \langle e_1, e_2, 0 | \rho_s(t) | e_1, e_2, 0 \rangle$ (blue line), and the probabilities of photon emission, $P(t)$ from state $|g_1, e_2, 1\rangle$ (cyan line), $Q(t)$ from state $|e_1, g_2, 1\rangle$ (black line), $R(t)$ from state $|g_1, g_2, 2\rangle$ (green line), and $R'(t)$ from state $|g_1, g_2, 1\rangle$ (red line) for $T = 10$ K. The parameters are in (a) the same as in Fig. 1(c) at two-photon resonance for $\Delta_2 = 2.6g_1\langle B \rangle$, in (b) the same as in Fig. 2(c) with $\Delta_2 = 2.4g_1\langle B \rangle$ corresponding to two-photon resonance, and in (c) and (d) the same as in Figs. 3(c) and 4(c), respectively, at two-photon resonance for $\Delta_2 = \Delta_1$.

the cavity-mode feeding process, followed by absorption of the phonon for negative detunings [17,22]. Therefore, when Δ_1 is fixed to a positive or negative value, the probabilities P , Q , and R become asymmetric along positive and negative values of Δ_2 .

In Fig. 5, we show evolution of the system after including electron-phonon interaction at $T = 10$ K. We plot the probability when both QDs are in the excited state $\rho_{ee}(t) = \langle e_1, e_2, 0 | \rho_s(t) | e_1, e_2, 0 \rangle$, single-photon emission probabilities $P(t) = \kappa \int_0^t d\tau \langle g_1, e_2, 1 | \rho_s(\tau) | g_1, e_2, 1 \rangle$, $Q(t) = \kappa \int_0^t d\tau \langle e_1, g_2, 1 | \rho_s(\tau) | e_1, g_2, 1 \rangle$, and $R(t) = 2\kappa \int_0^t d\tau \langle g_1, g_2, 2 | \rho_s(\tau) | g_1, g_2, 2 \rangle$. We also plot the probability $R'(t) = \kappa \int_0^t d\tau \langle g_1, g_2, 1 | \rho_s(\tau) | g_1, g_2, 1 \rangle$, when a photon is leaked from state $|g_1, g_2, 1\rangle$. For smaller values of spontaneous decay rate we find that $R'(t) = P(t) + Q(t) + R(t)$. First there is sharp rise in $R'(t)$ when the population in $|g_1, g_2, 1\rangle$ increases due to single-photon leakage from $|g_1, g_2, 2\rangle$, and then there is slow exponential growth to its maximum value when the transitions $|e_1, g_2, 0\rangle \rightarrow |g_1, g_2, 1\rangle$ and $|g_1, e_2, 0\rangle \rightarrow |g_1, g_2, 1\rangle$ take place. The probability ρ_{ee} follows rapid oscillations, and for smaller values of cavity damping, the average value decays exponentially. Figure 5(a) is obtained using the parameters of Fig. 1(c) and $\Delta_2 = 2.6g_1\langle B \rangle$, corresponding to the small cavity-induced two-photon resonance peak. In this case the value of $R(t)$ remains smaller than $Q(t)$, as the cavity-induced two-photon emission is smaller due to phonon interaction. In Fig. 5(b) we use the parameters of Fig. 2(c) and the value of Δ_2 corresponding to two-photon resonance at $\Delta_2 = 2.4g_1\langle B \rangle$. The probability R is larger than the probabilities P and Q , which shows that the phonon-induced cooperative two-photon transition from state $|e_1, e_2, 0\rangle$ dominates over individual single-photon transitions. Figures 2(c) and 2(d) are plotted for the parameters used in Figs. 3(c) and

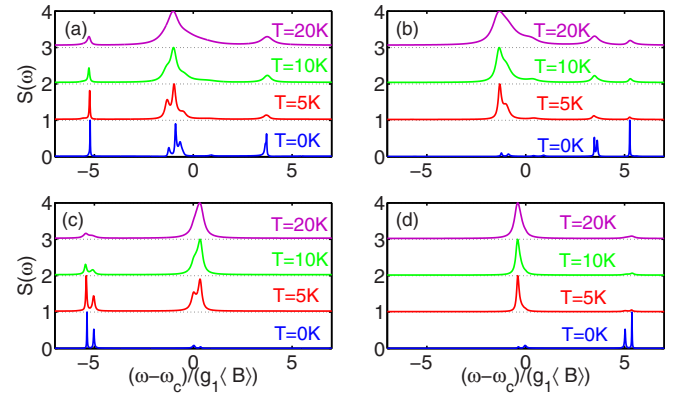


FIG. 6. The spectrum of photons emitted from the cavity mode for parameters the same as in Fig. 6 but for $T = 0, 5, 10,$ and 20 K.

4(c), respectively, and for $\Delta_2 = \Delta_1$ corresponding to phonon-induced two-photon resonance. We notice that for far off-resonant and equally detuned excitons, cooperative two-photon decay is dominating. Further, we find that cooperative decay is more pronounced for positive detuning $\Delta_1 = \Delta_2 = 5g_1\langle B \rangle$ [see Fig. 5(d)] than for negative detuning [see Fig. 5(c)]. Also, in Figs. 5(a) and 5(b), the oscillations in $\rho_{ee}(t)$ are more pronounced than in 5(c) and 5(d) because of stronger cavity interaction which results from larger values of g_2 and smaller values of $|\Delta_2|$.

In Fig. 6 we present a calculated cavity-mode spectrum $S(\omega) = \int_0^\infty dt \int_0^\infty d\tau a^\dagger(t)a(t+\tau) \exp(i\omega\tau)$. The two time correlation $a^\dagger(t)a(t+\tau)$ is calculated using quantum regression theorem. We use similar parameters as in Fig. 5 at different phonon bath temperatures. In order to accommodate four subplots for $T = 0, 5, 10,$ and 20 K, we normalize the maximum peak height to 1 by dividing all values with maximum value. The emitted spectrum can be understood using a dressed state picture of different excitation (number of excitons in QDs and number of photons in cavity mode) manifolds. The dressed state of two excitation manifold decay to dressed states of one excitation manifold and the dressed states of one excitation manifold decay to $|g_1, g_2, 0\rangle$. There are four dressed states in the two excitation manifold which are superpositions of $|e_1, e_2, 0\rangle, |g_1, e_2, 1\rangle, |e_1, g_2, 1\rangle,$ and $|g_1, g_2, 2\rangle$. There are three dressed states in the one excitation manifold which are superpositions of $|e_1, g_2, 0\rangle, |g_1, e_2, 0\rangle,$ and $|g_1, g_2, 1\rangle$. For $g_1, g_2 \ll \Delta_1, \Delta_2$, these dressed states are almost identical to the states of the composite system. Therefore, in principle there could be 15 peaks in the emission spectra, 12 from two excitation states and three peaks from single excitation states. However, for the parameter used in Fig. 6, only a few dominating peaks appear in the emission spectra. In Fig. 6(a) three narrower peaks appear from one excitation states, two centered around $\omega - \omega_c = \Delta_1, \omega - \omega_c = \Delta_2,$ and one centered around the cavity frequency (the middle peak among three overlapping peaks). The emitted spectrum from two excitation states contains emission from $|g_1, g_2, 2\rangle$ (broader right-hand side peak among the overlapping three peaks around the cavity frequency) and emission from individual QDs. The QDs are coupled with the cavity mode under the strong-coupling regime, and therefore the spectrum

of emitted photons from an individual QD has a doublet corresponding to an excitonlike and cavitylike frequency [7,25]. Two excitonlike peaks overlap with one excitation peak at $\omega - \omega_c \approx \Delta_1$, $\omega - \omega_c \approx \Delta_2$. Further, for far off-resonant QD the emission close to the cavity mode remains smaller. Two cavitylike peaks appear on either side of $\omega - \omega_c$, one along the negative side is a left-hand side peak among three overlapping peaks around cavity frequency, and the other on the positive side is not clearly visible. When the temperature of the phonon bath is raised the cavity-mode feeding increases, leading to a decrease in emission around exciton frequencies, and the emission around the cavity frequency increases. As a result, emission from both single-photon processes and cooperative two-photon processes appear around the cavity-mode frequency. In Figs. 6(b)–6(d), the cavity-induced two-photon processes are weak, and the emission is mainly from individual QDs for $T = 0$ K. Therefore, we get negligible emission around cavity frequency at $T = 0$ K. In Figs. 6(c) and 6(d), when QDs have the same coupling constants and detunings, in the spectrum emitted from one excitation states two peaks at $\omega - \omega_c \approx \Delta_1$, Δ_2 overlap for $T = 0$ K. Two additional peaks from two excitation states, one at $\omega - \omega_c = \Delta_1 = \Delta_2$ and another at cavity frequency, appear when the QDs emit in the presence of one photon in cavity mode. When the temperature is raised the emission around the cavity frequency dominates due to the increase in cavity-mode feeding and phonon-induced two-photon processes.

IV. CONCLUSIONS

We have predicted dominating two-photon emission from two off-resonantly coupled QDs in a photonic crystal cavity. We have found that when electron-phonon coupling is negligible, a cavity-induced two-photon transition could be dominating over single-photon transition if QDs are placed in the cavity such that their dipole coupling constant with cavity mode are not equal ($g_1 \neq g_2$) and their exciton transition frequencies satisfy the resonant condition $\Delta_1 + \Delta_2 + 2g_1^2/\Delta_1 + 2g_2^2/\Delta_2 \approx 0$. For QDs having the same dipole coupling constants ($g_1 = g_2$), cavity-induced two-photon transitions are negligible. In the presence of electron-phonon coupling, the cavity-induced two-photon transitions are strongly

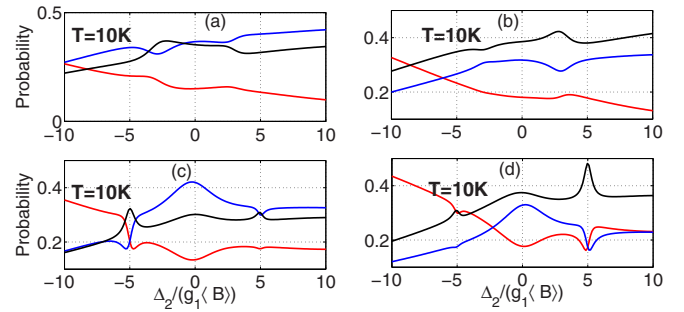


FIG. 7. The probabilities of photon emission, P from state $|g_1, e_2, 1\rangle$ (red line), Q from state $|e_1, g_2, 1\rangle$ (blue line), R from state $|g_1, g_2, 2\rangle$ (black line) using master equation (8). In (a) the parameters are the same as in Fig. 1(c), in (b) the parameters are the same as in Fig. 2(c), in (c) the parameters are the same as in Fig. 3(c), and in (d) the parameters are the same as in Fig. 4(c).

inhibited. However, phonon-induced two-photon transitions start dominating with a resonance for $\Delta_1 + 2g_1^2/\Delta_1 \approx \Delta_2 + 2g_2^2/\Delta_2$. On increasing temperature from 5 to 20 K, phonon-induced two-photon transitions increase, and for the red-detuned cavity-mode phonon-induced two-photon transitions start dominating at lower temperature than for the blue-detuned cavity mode. Our results can be used for realization of photonic systems when two or more QDs are integrated with the microcavity or waveguide.

ACKNOWLEDGMENT

We acknowledge financial support from SERB, Department of Science and Technology (DST), India [Project Grant No. SR/FTP/PS-122/2011].

APPENDIX: RESULTS OBTAINED USING SIMPLIFIED MASTER EQUATION (8)

In order to check the validity of the simplified master equation (8), we have plotted single-photon emission probabilities after integration of simplified master equation (8) using the same parameters of Figs. 1(c), 2(c) 3(c), and 4(c) in Fig. 7. The obtained results are a good match with all the features observed in Figs. 1–4.

-
- [1] R. H. Dicke, *Phys. Rev.* **93**, 99 (1954).
 - [2] M. Gross and S. Haroche, *Phys. Rep.* **93**, 301 (1982).
 - [3] R. Reimann, W. Alt, T. Kampschulte, T. Macha, L. Ratschbacher, N. Thau, S. Yoon, and D. Meschede, *Phys. Rev. Lett.* **114**, 023601 (2015); B. Casabone, K. Friebe, B. Brandstätter, K. Schüppert, R. Blatt, and T. E. Northup, *ibid.* **114**, 023602 (2015).
 - [4] R. G. DeVoe and R. G. Brewer, *Phys. Rev. Lett.* **76**, 2049 (1996).
 - [5] M. Scheibner, T. Schmidt, L. Worschech, A. Forchel, G. Bacher, T. Passow, and D. Hommel, *Nat. Phys.* **3**, 106 (2007); V. V. Temnov and U. Woggon, *Phys. Rev. Lett.* **95**, 243602 (2005).
 - [6] H.-R. Wei and F.-G. Deng, *Sci. Rep.* **4**, 7551 (2014).
 - [7] K. Hennessy, A. Badolato, M. Winger, D. Gerace, M. Atatüre, S. Gulde, S. Fält, E. L. Hu, and A. Imamoglu, *Nature (London)* **445**, 896 (2007).
 - [8] B.-S. Song, S. Noda, Takashi Asano, and Y. Akahane, *Nat. Mater.* **4**, 207 (2005); R. Benevides, Felipe G. S. Santos, Gustavo O. Luiz, Gustavo S. Wiederhecker, and Thiago P. Mayer Alegre, *Sci. Rep.* **7**, 2491 (2017).
 - [9] K. Tsuruda, M. Fujita, and T. Nagatsuma, *Opt. Express* **23**, 31977 (2015); E. Dulkeith, S. J. McNab, and Y. A. Vlasov, *Phys. Rev. B* **72**, 115102 (2005); S. J. McNab, N. Moll, and Y. A. Vlasov, *Opt. Express* **11**, 2927 (2003).

- [10] S. Weiler, A. Ulhaq, S. M. Ulrich, D. Richter, M. Jetter, P. Michler, C. Roy, and S. Hughes, *Phys. Rev. B* **86**, 241304(R) (2012); R. Oulton, J. J. Finley, A. I. Tartakovskii, D. J. Mowbray, M. S. Skolnick, M. Hopkinson, A. Vasanelli, R. Ferreira, and G. Bastard, *ibid.* **68**, 235301 (2003).
- [11] E. B. Flagg, A. Muller, J. W. Robertson, S. Founta, D. G. Deppe, M. Xiao, W. Ma, G. J. Salamo, and C. K. Shih, *Nat. Phys.* **5**, 203 (2009); E. B. Flagg, A. Müller, S. V. Polyakov, A. Ling, A. Migdall, and G. S. Solomon, *Phys. Rev. Lett.* **104**, 137401 (2010); S. Ates, S. M. Ulrich, S. Reitzenstein, A. Löffler, A. Forchel, and P. Michler, *ibid.* **103**, 167402 (2009); S. Ates, S. M. Ulrich, A. Ulhaq, S. Reitzenstein, A. Löffler, S. Hofling, A. Forchel, and P. Michler, *Nat. Photon.* **3**, 724 (2009).
- [12] J. P. Reithmaier, G. Sek, A. Löffler, C. Hofmann, S. Kuhn, S. Reitzenstein, L. V. Keldysh, V. D. Kulakovskii, T. L. Reinecke, and A. Forchel, *Nature (London)* **432**, 197 (2004); T. Yoshie, A. Scherer, J. Hendrickson, G. Khitrova, H. M. Gibbs, G. Rupper, C. Ell, O. B. Shchekin, and D. G. Deppe, *ibid.* **432**, 200 (2004); E. Peter, P. Senellart, D. Martrou, A. Lemaître, J. Hours, J. M. Gérard, and J. Bloch, *Phys. Rev. Lett.* **95**, 067401 (2005).
- [13] Y. Ota, S. Iwamoto, N. Kumagai, and Y. Arakawa, *Phys. Rev. Lett.* **107**, 233602 (2011); E. del Valle, A. Gonzalez-Tudela, E. Cancellieri, F. P. Laussy, and C. Tejedor, *New J. Phys.* **13**, 113014 (2011); S. Schumacher, J. Forstner, A. Zrenner, M. Florian, C. Gies, P. Gartner, and F. Jahnke, *Opt. Express* **20**, 5335 (2012); D. Heinze, A. Zrenner, and S. Schumacher, *Phys. Rev. B* **95**, 245306 (2017).
- [14] J. Kasprzak, S. Reitzenstein, E. A. Muljarov, C. Kistner, C. Schneider, M. Strauss, S. Höfling, A. Forchel, and W. Langbein, *Nat. Mater.* **9**, 304 (2010); C. Hopfmann, A. Carmele, A. Musiał, C. Schneider, M. Kamp, S. Höfling, A. Knorr, and S. Reitzenstein, *Phys. Rev. B* **95**, 035302 (2017).
- [15] B. Krummheuer, V. M. Axt, and T. Kuhn, *Phys. Rev. B* **65**, 195313 (2002); J. Forstner, C. Weber, J. Danckwerts, and A. Knorr, *Phys. Rev. Lett.* **91**, 127401 (2003); P. Borri, W. Langbein, S. Schneider, U. Woggon, R. L. Sellin, D. Ouyang, and D. Bimberg, *ibid.* **87**, 157401 (2001); M. Kaniber, A. Laucht, A. Neumann, J. M. Villas-Bôas, M. Bichler, M.-C. Amann, and J. J. Finley, *Phys. Rev. B* **77**, 161303(R) (2008); M. Winger, T. Volz, G. Tarel, S. Portolan, A. Badolato, K. J. Hennessy, E. L. Hu, A. Beveratos, J. Finley, V. Savona, and A. Imamoglu, *Phys. Rev. Lett.* **103**, 207403 (2009).
- [16] S. Hughes, P. Yao, F. Milde, A. Knorr, D. Dalacu, K. Mnaymneh, V. Sazonova, P. J. Poole, G. C. Aers, J. Lapointe, R. Cheriton, and R. L. Williams, *Phys. Rev. B* **83**, 165313 (2011); J. Xue, K.-D. Zhu, and H. Zheng, *J. Phys.: Condens. Matter* **20**, 325209 (2008); U. Hohenester, A. Laucht, M. Kaniber, N. Hauke, A. Neumann, A. Mohtashami, M. Seliger, M. Bichler, and J. J. Finley, *Phys. Rev. B* **80**, 201311(R) (2009); U. Hohenester, *ibid.* **81**, 155303 (2010).
- [17] I. Wilson-Rae and A. Imamoglu, *Phys. Rev. B* **65**, 235311 (2002); D. P. S. McCutcheon and A. Nazir, *New J. Phys.* **12**, 113042 (2010); C. Roy and S. Hughes, *Phys. Rev. X* **1**, 021009 (2011); *Phys. Rev. Lett.* **106**, 247403 (2011).
- [18] J. H. Quilter, A. J. Brash, F. Liu, M. Glässl, A. M. Barth, V. M. Axt, A. J. Ramsay, M. S. Skolnick, and A. M. Fox, *Phys. Rev. Lett.* **114**, 137401 (2015).
- [19] S. Bounouar, M. Müller, A. M. Barth, M. Glässl, V. M. Axt, and P. Michler, *Phys. Rev. B* **91**, 161302(R) (2015); M. Glässl, A. M. Barth, and V. M. Axt, *Phys. Rev. Lett.* **110**, 147401 (2013).
- [20] A. Laucht, J. M. Villas-Bôas, S. Stobbe, N. Hauke, F. Hofbauer, G. Böhm, P. Lodahl, M.-C. Amann, M. Kaniber, and J. J. Finley, *Phys. Rev. B* **82**, 075305 (2010); H. Kim, D. Sridharan, T. C. Shen, G. S. Solomon, and E. Waks, *Opt. Express* **19**, 2589 (2011).
- [21] A. Majumdar, M. Bajcsy, A. Rundquist, E. Kim, and J. Vučković, *Phys. Rev. B* **85**, 195301 (2012); M. Calic, C. Jarlov, P. Gallo, B. Dwir, A. Rudra, and E. Kapon, *Sci. Rep.* **7**, 4100 (2017).
- [22] S. M. Ulrich, S. Ates, S. Reitzenstein, A. Löffler, A. Forchel, and P. Michler, *Phys. Rev. Lett.* **106**, 247402 (2011).
- [23] S. M. Tan, *J. Opt. B* **1**, 424 (1999).
- [24] P. K. Pathak and G. S. Agarwal, *Phys. Rev. A* **70**, 043807 (2004).
- [25] S. Hughes and P. Yao, *Opt. Express* **17**, 3322 (2009).